Research, Society and Development, v. 10, n. 4, e44510414308, 2021
(CC BY 4.0) | ISSN 2525-3409 | DOI: http://dx.doi.org/10.33448/rsd-v10i4.14308

# Evaluation of X-shaped welded joints with Co-Cr alloy under different welding parameters: analysis by micro-CT and flexural strength

**Avaliação de juntas soldadas em forma de X com liga de Co-Cr sob diferentes parâmetros de soldagem: análise por micro-CT e resistência à flexão**

**Evaluación de uniones soldadas em forma de X con aleación de Co-Cr bajo diferentes parámetros de soldadura: análisis por micro-CT y resistencia a la flexión**

Received: 03/26/2021 | Reviewed: 04/02/2021 | Accept: 04/06/2021 | Published: 04/17/2021

**Morgana Guilherme de Castro Silverio**
ORCID: https://orcid.org/0000-0002-0352-7946
Universidade Federal de Uberlândia, Brazil
E-mail: morgana.guilherme@ufu.br
**Luís Henrique Araújo Raposo**
ORCID: https://orcid.org/0000-0003-2726-9133
Universidade Federal de Uberlândia, Brazil
E-mail: raposo@ufu.br
**Ricardo Tadeu Lopes**
ORCID: https://orcid.org/0000-0001-7250-824X
Universidade Federal do Rio de Janeiro, Brazil
E-mail: ricardo@lin.ufrj.br
**Paulo Cézar Simamoto Júnior**
ORCID: https://orcid.org/0000-0001-6087-9721
Universidade Federal de Uberlândia, Brazil
E-mail: psimamoto@ufu.br

**Abstract**
This study evaluated the mechanical strength correlated to the percentage of the total volume of weld and porosities of Co-Cr alloy joints welded with TIG technique. Thirty specimens were perpendicularly sectioned to the long-axis and rejoined by using X30-shaped joint design with TIG welding. They were divided into 3 groups (n=10): the CG1 with a 60-A depth and 90-ms pulse; the CG2 with a 60-A depth and 120-ms pulse and the CG3 with a 60-A depth and 160-ms pulse. The specimens were submitted to nondestructive tests: radiographic inspection, penetrant liquid and Micro-CT (to calculate the percentage of the total volume of welding and the porosities) and then tested with 3-point bending. The fracture surfaces were analyzed with scanning electron microscopy (SEM). The data were statistically analyzed with 1-way ANOVA and the Tukey post hoc test for all the variables which were analyzed: flexural strength, total volume of weld and porosities. Pearson correlation test was also applied (α=.05). The 1-way ANOVA showed that the factors machine parameters were not significant for flexural strength values (P=.231), the total volume of weld (P=.057) and porosities (P=.057). There are no significant relationships between any pair of variables after Pearson correlation test (P >.050). This, suggesting that the three machine regulation can be an option for joining prefabricated Co-Cr rods in this kind of union.
**Keywords:** Dental alloys; Dental soldering; Flexural strength.

**Resumo**
Este estudo avaliou a resistência mecânica, correlacionada ao percentual do volume total de solda e porosidades, de juntas soldadas de Co-Cr com a técnica TIG em diferentes regulagens do equipamento. Trinta amostras foram seccionadas perpendicularmente e unidas com soldagem TIG com junta em forma de X. Estas foram divididas em 3 grupos (n = 10): CG1 com profundidade de 60-A e pulso de 90 ms; CG2 com profundidade de 60 A e pulso de 120 ms e CG3 com profundidade de 60 A e pulso de 160 ms. As amostras foram submetidas a ensaios não destrutivos (inspeção radiográfica, líquido penetrante e Micro-CT (para cálculo do percentual do volume total de soldagem e das porosidades)) e ensaio de flexão em 3 pontos. As superfícies das fraturas foram analisadas em microscopia eletrônica de varredura (MEV). Os dados foram analisados estatisticamente com ANOVA one way e teste post hoc de Tukey para todas as variáveis analisadas: resistência à flexão, volume total de solda e porosidades. O teste de correlação de Pearson também foi aplicado (α = 0,05). ANOVA one way mostrou que os fatores regulagem do equipamento não foram significativos para os valores de resistência à flexão (P = .231), volume total de solda (P = .057) e porosidades (P = .057). Não houve relações significativas entre qualquer par de variáveis após o teste de correlação de Pearson (P>

0,050). Isso sugere que as três regulagens do equipamento podem ser uma opção para unir barras pré-fabricadas de Co-Cr neste tipo de união.
**Palavras-chave:** Ligas metálicas; Soldagem dentária; Resistência à flexão.

**Resumen**
Este estudio evaluó la resistencia mecánica, correlacionada con el porcentaje del volumen total de soldadura y la porosidad, de las uniones soldadas con Co-Cr con la técnica TIG en diferentes configuraciones del equipo. Treinta muestras se seccionaron perpendicularmente y se unieron con soldadura TIG con junta en forma de X. Se dividieron en 3 grupos (n = 10): el CG1 con una profundidad de 60 A y un pulso de 90 ms; el CG2 con una profundidad de 60 A y pulso de 120 ms y el CG3 con una profundidad de 60 A y un pulso de 160 ms. Las muestras fueron sometidas a ensayos no destructivos (inspección radiográfica, líquido penetrante y Micro-CT (para calcular el porcentaje del volumen total de soldadura y las porosidades)) y ensayados con flexión de 3 puntos. Las superficies de fractura se analizaron con microscopía electrónica de barrido (SEM). Los datos se analizaron estadísticamente con ANOVA one way y el test post hoc de Tukey para todas las variables analizadas: resistencia a la flexión, volumen total de soldadura y porosidades. También se aplicó la prueba de correlación de Pearson (α = .05). ANOVA one way mostró que los factores parámetros de la máquina no fueron significativos para los valores de resistencia a la flexión (P = .231), el volumen total de soldadura (P = .057) y las porosidades (P = .057). No hay relaciones significativas entre ningún par de variables después de la prueba de correlación de Pearson (P> .050). Esto sugiere que las tres configuraciones del equipo pueden ser una opción para unir barras de Co-Cr prefabricadas en este tipo de unión.
**Palabras clave:** Aleaciones dentales; Soldadura dental; Fuerza flexible.

## 1. Introduction

Implantology focused on the oral rehabilitation of edentulous patients has been well-documented and extensively performed, with high success rates. This rehabilitation model, which became known *ad modum* as the Brånemark Protocol, has been the subject of several studies, both in relation to implants and with respect to the metallic framework (Lyra e Silva, et al. 2012; Silveira-Júnior, et al. 2012; Castro, et al. 2015; Simamoto-Júnior et al., 2015).

The studies focused on prosthetic frameworks were developed to optimize their production by the use of prefabricated bars and welding techniques other than conventional welding (Lyra e Silva, et al. 2012; Silveira-Júnior, et al. 2012; Castro, et al. 2015; Simamoto-Júnior, et al., 2015). Studies have been conducted to evaluate the types of welding techniques (Wang & Welsch, 1995; Baba & Watanabe, 2005; Rocha, et al. 2006; Zupancic, et al. 2006; Barbi, et al. 2012; Lyra e Silva, et al. 2012; Nuñez-Pantoja, et al. 2012; Atoui, et al. 2013; Castro, et al. 2013; Castro, et al. 2015; Matos, et al. 2015; Simamoto-Júnior, et al. 2015), the settings of welding equipment (Chai & Chou, 1998; Baba & Watanabe, 2005; Akman, et al. 2009; Lyra e Silva, et al. 2015), the types of alloys used (Rocha, et al. 2006; Watanabe & Topham, 2006; Takayama, et al. 2012; Takayama, et al. 2013; Lyra e Silva, et al. 2015; Matos, et al. 2015), the settings of the joints (Zupancic, et al. 2006; Nuñez-Pantoja, et al. 2012; Takayama, et al. 2012; Kokolis, et al. 2015; Simamoto-Júnior, et al. 2015), and mechanical methods of evaluation of these weld joints (Nuñez-Pantoja, et al. 2011; Takayama, et al. 2012; Takayama, et al. 2013; Castro, et al. 2015).

Among the welding techniques, two have been identified for dental use: laser welding (Berg, et al. 1995; Wang and Welsch, 1995; Chai & Chou, 1998; Baba & Watanabe, 2005; Akman, et al. 2009; Byrne, 2011; Nuñez-Pantoja, et al. 2011; Barbi, et al. 2012; Nuñez-Pantoja, et al. 2012; Silveira-Júnior, et al. 2012; Takayma, et al. 2012; Atoui, et al. 2013; Castro, et al. 2013; Takayama, et al. 2013; Castro, et al. 2015; Kokolis, et al. 2015; Matos, et al. 2015) and TIG or plasma welding (Wang & Welsch, 1995; Taylor, et al. 1998; Rocha, et al. 2006; Byrne, 2011; Barbi, et al. 2012; Lyra e Silva, et al. 2012; Nuñez-Pantoja, et al. 2012; Silveira-Júnior, et al. 2012; Atoui, et al. 2013; Castro, et al. 2013; Castro, et al. 2015; Matos, et al. 2015; Simamoto-Júnior, et al. 2015). Both have some advantages: welding can be performed directly on the model (Chai & Chou, 1998; Baba & Watanabe, 2005; Rocha, et al. 2006; Zupancic, et al. 2006; Barbi, et al. 2012; Silveira-Júnior, et al. 2012; Castro, et al. 2015), energy can be concentrated in a small area (Rocha, et al. 2006; Barbi, et al. 2012; Lyra e Silva, et al. 2012; Silveira-Júnior, et al. 2012; Takayama, et al. 2013; Castro, et al. 2015), resulting in a reduced HAZ (Heat affected zone) (Baba & Watanabe, 2005; Nuñez-Pantoja, et al. 2011; Silveira-Júnior, et al. 2012; Castro, et al. 2015) although laser welding has an

even smaller HAZ than TIG welding (Atoui, et al. 2013; Castro, et al. 2015), allowing for repair in regions close to the resin and ceramic (Chai & Chou, 1998; Baba & Watanabe, 2005; Rocha, et al. 2006; Zupancic, et al. 2006; Nuñez-Pantoja, et al. 2011; Nuñez-Pantoja, et al. 2012; Silveira-Júnior, et al. 2012; Castro, et al. 2015; Kokolis, et al. 2015), good finish weld pool, the possibility for welding in any position (Silveira-Júnior, et al. 2012; Castro, et al. 2015), and less time required compared with that needed for conventional welding (Baba & Watanabe, 2005; Rocha, et al. 2006; Zupancic, et al. 2006; Silveira-Júnior, et al. 2012; Castro, et al. 2015; Kokolis, et al. 2015). The decision regarding how a welding technique will be used should be based on the availability of equipment (Barbi, et al. 2012). However, the cost of equipment is markedly different between techniques, with the laser welding equipment being much more expensive than the TIG equipment and often unavailable for use by the prosthesis-manufacturing laboratories (Silveira-Júnior, et al. 2012; Atoui, et al. 2013; Castro, et al. 2015).

Regardless of the technique used, studies have shown that the welding machine configuration appears to exert influence on the welding process. Studies have been developed to investigate the influence of parameters such as: current density or electric voltage (peak power) (Chai & Chou, 1998; Baba & Watanabe, 2005; Akman, et al. 2009), pulse duration (Chai & Chou, 1998; Baba & Watanabe, 2005; Akman, et al. 2009; Lyra e Silva, et al. 2012; Takayama, et al. 2013), the diameter of the spot weld (Baba & Watanabe, 2005; Akman, et al. 2009; Takayama, et al. 2013), and the use of the argon shield (Watanabe & Topham, 2006; Akman, et al. 2009; Takayama, et al. 2012) in penetration depth.

Akman et al. 2009 studied the effects of different parameters on the laser welding of Ti-6Al-4V specimens in relation to penetration depth and concluded that peak power was the most important parameter, but if that power was increased too much, the temperature of the workpiece exceeded the evaporation point of the alloy and promoted crater formation on the surface of the material. To increase penetration depth without craters, pulse duration was increased and thus the width of the heat-affected zone, the weld pool, was increased at the same penetration depth.

The type of alloy has also been studied (Rocha, et al. 2006; Watanabe & Topham, 2006; Lyra e Silva, et al. 2012; Takayama, et al. 2012; Takayama, et al. 2013). While titanium alloys are most often used in studies because of their advantages of good compatibility, low density, and anti-corrosion properties (Berg, et al. 1995; Chai & Chou, 1998; Taylor, et al. 1998; Rocha, et al. 2006; Akman, et al. 2009; Nuñez-Pantoja, et al. 2011; Lyra e Silva, et al. 2012; Silveira-Júnior, et al. 2012; Takayama, et al. 2012; Atoui, et al. 2013; Takayama, et al. 2013; Castro, et al. 2015; Simamoto-Júnior, et al. 2015), casting and welding these alloys can be difficult, since titanium, when subjected to high temperatures, has high oxygen, nitrogen, and hydrogen reactivity and can become contaminated, leaving the welded areas of the framework more vulnerable (Berg, et al. 1995; Wang & Welsch, 1995; Chai & Chou, 1998; Taylor, et al. 1998; Lyra e Silva, et al. 2012; Silveira-Júnior, et al. 2012; Castro, et al. 2015; Akman, et al. 2009; Nuñez-Pantoja, et al. 2011; Nuñez-Pantoja, et al. 2012; Takayama, et al. 2012; Atoui, et al. 2013; Simamoto-Júnior, et al. 2015). Moreover, Co-Cr alloys are increasingly popular in prosthetic dentistry, due to a favorable combination of biocompatibility, resistance to corrosion, castability, weight, stiffness, and low cost (Rocha, et al. 2006; Zupancic, et al. 2006; Barbi, et al. 2012; Kokolis, et al. 2015).

The configuration of the joint is another factor influencing the resistance of welded joints (Nuñez-Pantoja, et al. 2011; Nuñez-Pantoja, et al. 2012; Takayama, et al. 2013; Castro, et al. 2015; Kokolis, et al. 2015; Simamoto-Júnior, et al. 2015). Castro, et al. 2015 evaluated the mechanical strength of Ti-6Al-4V alloy frameworks with samples of different diameters with an I-shaped joint configuration welded with both laser and plasma techniques. They found that there was incomplete penetration in all samples and that the internal void left thereby may have been one of the main reasons for the decreased strength in the welded joints. Similar results were found by Zupancic, et al. 2006 and Kokolis, et al. 2015 in I-shaped joints of Co-Cr subjected to laser welding.

Simamoto-Júnior, et al (2015) proposed the use of welded joints in X-shaped frameworks, which greatly improved their mechanical behavior. TIG welding associated with the X-shaped design resulted in higher joint resistance, similar to that

of the control group. Furthermore, in the same study, they evaluated two different angles of this type of chamfer and concluded that an X-shaped design with a 60-degree chamfer had better strength values than designs with a 45-degree chamfer. Contrary results were found by Zupancic, et al. 2006 in laser-welded Co-Cr samples in which the change in the configuration of the joint to an X-shape did not increase resistance values.

Finally, in joint evaluations, investigators have been increasingly attempting to understand the mechanical behavior of welded frameworks and propose improvements in welding processes. Therefore, most studies have used non-destructive tests such as radiographic evaluation (Rocha, et al. 2006; Nuñez-Pantoja, et al. 2011; Lyra e Silva, et al. 2012; Nuñez-Pantoja, et al. 2012; Simamoto-Júnior, et al. 2015) as well as destructive tests with the ultimate tensile test (Berg, et al. 1995; Wang & Welsch, 1995; Chai & Chou, 1998; Taylor, et al. 1998; Watanabe & Topham, 2006; Zupancic, et al. 2006; Akman, et al. 2009; Takayama, et al. 2012; Atoui, et al. 2013; Takayama, et al. 2013; Castro, et al. 2015), and bending test (Rocha, et al. 2006; Lyra e Silva, et al. 2012; Atoui, et al. 2013; Simamoto-Júnior, et al. 2015). However, few studies have used tests such as evaluation by micro-CT (Takayama, et al. 2012; Takayama, et al. 2013) and evaluation by the finite element method (Castro, et al. 2015). Among these, micro-CT facilitates the 3-dimensional evaluation of all welded inner areas, allowing for the identification and calculation of porosities and internal voids (Takayama, et al. 2012; Takayama, et al. 2013) and for the evaluation and calculation of solder volume in the joint.

The purpose of this study was evaluation of the mechanical strength of a Co-Cr alloy in different machine regulations of the TIG technique by the application of micro-CT (for calculation of the percentage of the total volume of weld and porosities) and the 3-point bending test. Two hypotheses were tested: the first, that differences would be found between the machine regulations in relation to flexural strength and total volume of weld but not in relation to porosities; and the second, that there would be positive correlation between the flexural strength and total volume of weld and between the flexural strength and porosities for all groups.

## 2. Material and Methods

Thirty Co-Cr alloy bar specimens were sectioned perpendicular to the long axis and re-joined in an X30-shaped joint design (3.18 mm in diameter × 40.0 mm in length) (Figure 1) with TIG welding and divided into 3 groups (n=10): CG1, with a 60-Å depth (current density) and 90-ms pulse (continuous arc); CG2, with a 60-Å depth and 120-ms pulse; and CG3, with a 60-Å depth and 160-ms pulse. For construction of the specimen design, segments were milled at their extremities with a lathe (PRN-320; IMOR), producing 1-mm-deep X-shaped chamfers with 30-degree angles between the bar extremities (Zupancic, et al. 2006; Barbi, et al. 2012; Simamoto-Júnior, et al. 2015).

**Figure 1.** Geometry of specimens in X-shaped joint design with 30-degree chamfer.

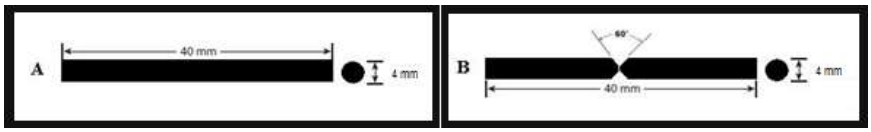


Source: Authors.

For standardization, the specimens were fixed in a holding matrix to ensure that both halves were properly aligned and juxtaposed during welding procedures (Lyra e Silva, et al. 2012; Simamoto-Júnior, et al. 2015). TIG welding was performed with specific dental equipment (NTY60C; Kernit) set to 60-Å depth and pulse range according to group. The electrode was placed perpendicular to the segment to be welded at a .5-mm distance, as recommended by the manufacturer. Two opposite welding points were initially made, connecting the central part of the joint and stabilizing the specimens. The

framework was then removed from the matrix to facilitate the welding of the entire circumference (Castro, et al. 2015). After every 2 welds, the electrode was cleaned to ensure adequate performance. The argon gas flow rate was set to 10 L/min, and the flow began 2 seconds before and ended 2 seconds after the welding procedure to allow the specimens to cool in an inert atmosphere (Simamoto-Júnior, et al. 2015). TIG welding was performed by the same operator (L.R. Miranda).

After the welding procedures, the welded regions were evaluated radiographically (Timex 70; Gnatus) by digital imaging (X-Scan Duo; Air Techniques) for the detection of defects, represented by radiolucent points at the joints. Additionally, a dye-revealing liquid (VP 30; Metal-Chek) was applied for the detection of surface failure (Nuñez-Pantoja, et al. 2011; Simamoto-Júnior, et al. 2015). Specimens that showed failure were discarded and replaced.

The welded areas of all specimens were observed by means of a micro-CT device (SkyScan1173, Bruker micro-CT NV Belgium). The tube voltage was 130 kV for the Co–Cr alloy; the current produced by the X-ray generator was 61 Å. X-ray image acquisition was performed with a CCD camera equipped with the micro-CT device. In total, 517 slices of the welded areas of the specimens were obtained vertically along the lengths of the specimens. The thickness of each slice was .016 mm. These images were reconstructed by cross-section images from tomography projection images (SkyScan NRecon; Bruker micro-CT NV Belgium), and then 3-dimensional models were constructed with the use of image analysis software (CT-Analyser [CTAn]; Bruker micro-CT NV Belgium). The sizes, numbers, and total volume ratios of welding and the bubbles and spaces present in the specimens were also determined with the software. The percentage of total welding volume was calculated based on the entire welded area, including the bubbles and spaces. The percentage of porosities was calculated from the total volume ratios of the bubbles and the spaces (Takayama, et al. 2012).

Specimens were tested for flexural strength in 3-point bending design with 3-mm-diameter rods and 20-mm span-length between supports. Compressive loading was applied at .5 mm/min crosshead speed with a 3-mm-diameter rod positioned at the center of the specimen. The test was considered finished when any sudden loading change (load drop) representing failure or permanent deformation of the beam was detected, until a maximum displacement of 5 mm. The flexural strength (MPa) of the specimens was obtained according to the following equation: $fs=8FL/\pi D^3$, where fs is the flexural strength (MPa), F is the value of fracture strength or elastic limit (N), L is the distance between supports, and D is the diameter of the specimen (mm) (Lyra e Silva, et al. 2012; Simamoto-Júnior, et al. 2015).

Since the specimens in each group had similar fracture patterns, 3 specimens of each group were subjected to SEM at ×20, ×50, ×100, ×200, and ×500 magnification, and those images that were most representative were used to demonstrate the failure pattern characteristics (JSM 5600LV; JEOL).

The data were statistically analyzed, separately, with 1-way ANOVA and the Tukey post hoc test for all variables analyzed: flexural strength and total volume of weld and porosities. The Pearson correlation test was used to correlate the flexural strength and total volume of weld and to correlate the flexural strength and porosities for all groups ($\alpha$=.05 for all statistical tests).

## 3. Results

Mean and standard deviation values for Flexural strength (MPa), total volume of weld (%) and porosities (%) in each tested group are shown in Table 1.

**Table 1.** Mean and standard deviations (SD) for Flexural strength (MPa), total volume of weld (%) and porosities (%), and statistical categories defined by Tukey test.

| Groups | Flexural Strength (MPa) Mean ±SD | Total volume of weld (%) Mean ±SD | Porosities (%) Mean ±SD |
|---|---|---|---|
| CG1 | 1536.2 ±278.9$^{A}$ | 99.7 ±0.1$^{A}$ | 0.3 ±0.1$^{A}$ |
| CG2 | 1679.8 ±235.7$^{A}$ | 99.6 ±0.2$^{A}$ | 0.4 ±0.2$^{A}$ |
| CG3 | 1507.5 ±177.9$^{A}$ | 99.3 ±0.7$^{A}$ | 0.7 ±0.7$^{A}$ |

Source: Authors.

Different capital letters in table 1 represent significant difference identified by Tukey HSD test for different groups in each parameter (P<.05). This means, that there was no statistically significant difference between the groups analyzed in this work for none of the analyzed parameters.

**Table 2.** One-way ANOVA for flexural strength values (MPa) of groups.

| Source of variation | Df | Sum of Square | Mean square | F | P |
|---|---|---|---|---|---|
| Between groups | 2 | 170439 | 85219 | 1.550 | .231 |
| Residual | 27 | 1484829 | 54993 | | |
| Total | 29 | 1655269 | | | |

Source: Authors.

Table 2 present the 1-way ANOVA statistical test that showed that machine regulation factors (P=.231) were not significant for flexural strength values.

**Table 3.** One-way ANOVA for total volume of weld values (%) of groups.

| Source of variation | df | Sum of square | Mean square | F | P |
|---|---|---|---|---|---|
| Between groups | 2 | .185 | .0924 | 1.306 | .287 |
| Residual | 27 | 1.911 | .0708 | | |
| Total | 29 | 2.096 | | | |

Source: Authors.

Table 3 present the 1-way ANOVA statistical test for total volume of weld, and showed that the machine regulation factors (P=.287) were not significant.

**Table 4.** One-way ANOVA for porosities values (%) of groups.

| Source of variation | df | Sum of square | Mean square | F | P |
|---|---|---|---|---|---|
| Between groups | 2 | .184 | .0921 | 1.300 | .289 |
| Residual | 27 | 1.913 | .0709 | | |
| Total | 29 | 2.097 | | | |

Source: Authors.

Table 4 present the 1-way ANOVA statistical test for porosity, and showed that the machine regulation factors (P=.289) were not significant.

There were no significant relationships between pairs of variables after the Pearson correlation test (P>.050).

Figures 2 and 3 are micro-CT images of the welded area, and Figures 4 and 5 are SEM images of the fractured welded area.

**Figure 2.** Micro-CT image of specimen from CG1.

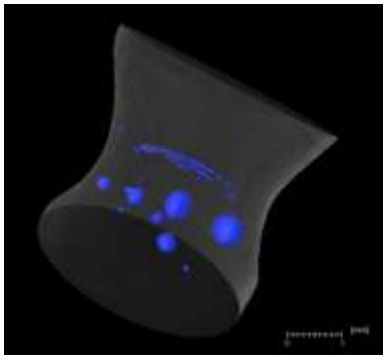

Source: Authors.

**Figure 3.** Micro-CT image of specimen from CG2.

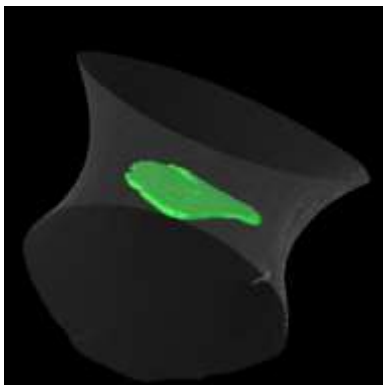

Source: Authors.

Figures 2 and 3 show the total volume of the welded area and the porosities (bubbles and spaces) inside the welded area pointed out by the blue and green structures in the respective figures.

**Figure 4.** Scanning electron microscope images at ×20 magnification of specimen from CG3.

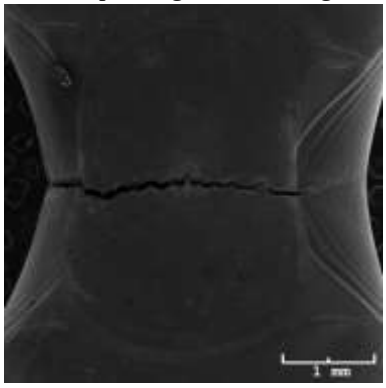

Source: Authors.

**Figure 5.** Scanning electron microscope images at ×500 magnification of specimen from CG2.

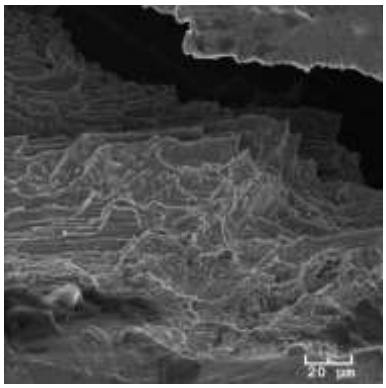

Source: Authors.

Figures 4 and 5 show the failure pattern characteristics. Figure 4 shows partial fracture in the welded region, and Figure 5 presents a fairly flat overall surface with shallow dimples, indicating ductility of the fracture.

## 4. Discussion

The first hypothesis tested — that differences would be found between the machine regulation in relation to both flexural strength and total volume of weld — was rejected, and the second hypothesis — that no differences would be found in relation to porosities — was accepted. The 1-way ANOVA showed that machine regulation factors (P=.231) were not significant for flexural strength values, for total volume of weld, and for porosity (P=.289).

Several factors could account for this result, such as welding technique,(Berg, et al. 1995; Wang & Welsch, 1995; Chai & Chou, 1998; Baba & Watanabe, 2005; Rocha, et al. 2006; Watanabe & Topham, 2006; Zupancic, et al. 2006; Akman, et al. 2009; Barbi, et al. 2012; Nuñez-Pantoja, et al. 2011; Lyra e Silva, et al. 2012; Silveira-Júnior, et al 2012; Takayama, et al. 2012; Takayama, et al. 2013; Castro, et al. 2015; Matos, et al. 2015; Simamoto-Júnior, et al. 2015) the variations in the welding parameters of the equipment used (Chai & Chou, 1998; Baba & Watanabe, 2005; Watanabe & Topham, 2006; Akman, et al. 2009; Lyra e Silva, et al. 2012; Takayama, et al. 2012; Takayama, et al. 2013), the presence of porosities and internal voids (Berg, et al. 1995; Wang & Welsch, 1995; Chai & Chou, 1998; Watanabe & Topham, 2006; Zupancic, et al. 2006; Nuñez-Pantoja, et al. 2011; Lyra e Silva, et al. 2012; Nuñez-Pantoja, et al. 2012; Takayama, et al. 2012; Takayama, et al. 2013; Castro, et al. 2015; Kokolis, et al. 2015; Simamoto-Júnior, et al. 2015), welder experience (Takayama, et al. 2012; Castro, et al. 2013; Takayama, et al. 2013; Kokolis, et al. 2015), and the correct sharpening of the tungsten electrode (Castro, et al. 2015;

Simamoto-Júnior, et al. 2015).

In TIG welding, the heating of metal is too highly localized by a plasma arc established between the non-consumable electrode and the workpiece to be welded, leading to melting of the base metal (Wang & Welsch, 1995; Taylor, et al. 1998; Rocha, et al. 2006; Barbi, et al. 2012; Lyra e Silva, et al. 2012; Nuñez-Pantoja, et al. 2012; Silveira-Júnior, et al. 2012; Atoui, et al. 2013; Castro, et al. 2013; Castro, et al. 2015; Simamoto-Júnior, et al. 2015), generating welded joints with good finish (mainly in small-diameter structures (Silveira-Júnior, et al. 2012; Castro, et al. 2015)), and therefore, since the samples were of the same diameter (3.18 mm), metal fusion was similar in all groups, which was confirmed by micro-CT images (e.g. Figures 1 and 2) showing similar weld volumes in the different samples of different groups. Further, the measurement of the weld volume showed no statistically significant difference between groups (P=.287) (Table 1).

Under optimal welding conditions, the resistance of welded joints should be equivalent to that of unwelded samples (Berg, et al. 1995; Chai & Chou, 1998; Taylor, et al. 1998; Castro, et al. 2015); however, incomplete penetration could generate internal porosities and voids that could be significant weakening factors (Berg, et al. 1995; Wang & Welsch, 1995; Chai & Chou, 1998; Zupancic, et al. 2006; Nuñez-Pantoja, et al. 2011; Lyra e Silva, et al. 2012; Nuñez-Pantoja, et al. 2012; Atoui, et al. 2013; Castro, et al. 2015; Kokolis, et al. 2015; Simamoto-Júnior, et al. 2015). This incomplete penetration may result from several factors, such as: the cooling and solidification of the metal after being welded (Takayama, et al. 2013), altering the mechanical, physical, and chemical properties of metal (Atoui, et al. 2013; Castro, et al. 2015); vaporization of volatile alloying elements (Nuñez-Pantoja, et al. 2012); or regulation of the welding machine parameters (Chai & Chou, 1998; Baba & Watanabe, 2005; Watanabe & Topham, 2006; Akman, et al. 2009; Lyra e Silva, et al. 2012; Nuñez-Pantoja, et al. 2012; Takayama, et al. 2013). Among the parameters that can be adjusted are current density or electric voltage (peak power) (Chai & Chou, 1998; Baba & Watanabe, 2005; Akman, et al. 2009), pulse duration (Chai & Chou, 1998; Baba & Watanabe, 2005; Akman, et al. 2009; Lyra e Silva, et al. 2012; Takayama, et al. 2013), the diameter of the spot weld (Baba & Watanabe, 2005; Akman, et al. 2009; Takayama, et al. 2013), and the use of an argon shield (Watanabe & Topham, 2006; Akman, et al. 2009; Takayama, et al. 2012).

Chai and Chou, 1998 evaluated the mechanical properties of commercially pure Ti subjected to laser welding under different conditions to determine the best welding parameters relative to voltage and pulse duration. They found that there was no statistically significant difference in the pulse duration factors for UTS values and concluded that voltage was the only factor that affected the resistance values of welded samples. Baba and Watanabe, 2005 examined the penetration depth into different casting alloys under several laser welding conditions. They concluded that when the voltage increased and the spot diameter decreased, the penetration depth increased for each metal. Similar values were found by Lyra e Silva, et al. 2012, who reported that the variations in pulse duration on the plasma welding machine showed no statistically significant difference when the same current was maintained for samples of Ti-6Al-4V in the flexural strength test.

Therefore, since, in the present study, the same current of 60 Å was used and only the pulse duration varied (90, 120, and 160 ms), the results are similar to those obtained in the aforementioned studies. The 1-way ANOVA showed that machine regulation factors (P=.231) were not significant for flexural strength values.

Moreover, it is possible that, in this study, the porosities and internal voids were also the result of inclusion of the shielding gas (argon or helium) used in the TIG welding technique (Akman, et al. 2009; Nuñez-Pantoja, et al. 2011; Nuñez-Pantoja, et al. 2012; Silveira-Júnior, et al. 2012; Castro, et al.2015; Simamoto-Júnior, et al. 2015) and/or incomplete weld penetration, also caused by the shielding gas (Watanabe & Topham, 2006). Although in this work an X-shaped joint was used, which favors greater weld penetration (Nuñez-Pantoja, et al. 2012; Simamoto-Júnior, et al. 2015), different from that of I-shaped joints that confine welding to only the periphery of the sample, generating a large internal void (Zupancic, et al. 2006; Nuñez-Pantoja, et al. 2012; Castro, et al. 2015; Simamoto-Júnior, et al. 2015), it can be detected on the micro-CT images (e.g.

Figures 2 and 3) that all samples had porosities and internal voids and all fractured in the welded region (Figure 4). Watanabe and Thopam, 2006 investigated the effect of argon shielding gas on the resistance of laser-welded joints in different alloys, among them the Co-Cr alloy, and concluded that, at a constant current of 220 V and a pulse duration of 10 ms, the samples welded without the shielding gas showed resistance values higher than those of samples welded in the presence of gas. This is because the oxidation of Co-Cr is limited to the sample surface, favoring the penetration of the weld into the interior of the alloy. Takayama, et al. 2012 used micro-CT to evaluate the porosities of laser-welded Co-Cr samples with different flow rates of protective gas and found that the greater the amount of gas, the higher the number of porosities. Therefore, it is likely that porosities and internal voids were the result of the inclusion of the shielding gas and incomplete weld penetration caused by the gas itself. These porosities and internal voids acted as stress concentration points and led the structures to fail in the welded region during destructive tests (Wang & Welsch, 1995; Chai & Chou, 1998; Nuñez-Pantoja, et al. 2012; Castro, et al. 2015; Simamoto-Júnior, et al. 2015).

Thus, in ideal situations, welded areas should behave as do base metals (Berg, et al. 1995; Chai & Chou, 1998; Rocha, et al. 2006; Castro, et al. 2015), and breakage could occur, or not, in any region of the cross-section (Berg, et al. 1995; Chai & Chou, 1998; Rocha, et al. 2006; Castro, et al. 2015) or there would be only metal plastic deformation, because of the type of mechanical test used in this study – 3-point bend test with a 5-mm deformation limit and collapse of 20%. However, all samples broke at the welding joint, which led to the conclusion that these porosities actually led to the failure of the welded joint (Berg, et al. 1995; Chai & Chou, 1998; Zupancic, et al. 2006; Nuñez-Pantoja, et al. 2012; Castro, et al. 2015; Simamoto-Júnior, et al. 2015).

Moreover, the fact that the second hypothesis of this work was rejected (there were no significant relationships between pairs of variables after the Pearson correlation test [P >.050]) leads to two conclusions: The first, given independent quantitative differences or sizes of porosities and internal voids, means that the simple fact of the existence of a porosity indicates stress concentration at this point, with crack propagation leading to failure in these regions (Zupancic, et al. 2006; Nuñez-Pantoja, et al. 2012; Silveira-Júnior, et al. 2012; Castro, et al. 2015; Simamoto-Júnior, et al. 2015). The second is that the weld volume had no positive correlation with resistance values and possibly a larger volume of solder in all specimens would not change this statistical results. This conclusion has been reached since, in this work, welded metal was not added, causing a constriction in the welded region (Figures 2, 3, and 4), although the TIG welding technique permits its use (Nuñez-Pantoja, et al. 2012; Silveira-Júnior, et al. 2012; Matos, et al. 2015; Simamoto-Júnior, et al. 2015).

Regarding the welder, some authors (Takayama, et al. 2012; Castro, et al. 2013; Takayama, et al. 2013; Kokolis, et al. 2015) claimed that different welders and their levels of experience can also influence the weld quality, but in this present work a single experienced welder welded all samples at one sitting, and therefore it is possible that the effects of this variable were minimized. Regarding the sharpening of the electrode, the tungsten electrode should be kept sharpened, in accordance with the manufacturer's specifications, before each new spot weld to improve the quality of the welded joint (Castro, et al. 2015; Simamoto-Júnior, et al. 2015). Since this was achieved in this work, it is likely that this variable had no influence on the results.

Moreover, there are limitations to the longevity of these structures; therefore, aging tests such as corrosion behavior (Zupancic, et al. 2006; Matos, et al. 2015) and fatigue tests (Nuñez-Pantoja, et al. 2012) should be conducted to assess this condition. In addition, studies in which these structures were applied to the cylinder fabricating the bars for clinical use are necessary to evaluate longevity in relation to the cylinder in a complete framework (Zupancic, et al. 2006).Further studies in relation to masticatory forces exerted by patients on these structures are also necessary to establish benchmarks for comparison with the values obtained in this and other studies.

## 5. Conclusions

Within the limitations of this research and after the finding that the machine parameter is only one aspect to be considered in evaluation of the success of welding techniques, the three different machine parameters used in this work can be regarded as options for joining prefabricated bars in prosthetic frameworks by TIG welding in terms of the configuration of the joints used in this study. Other studies should be developed with the same methodologies to evaluate not only welding processes but also casting processes, with other metal alloys and with different diameters.

## Acknowledgments

The authors would like to thank the support of CNPQ. The project was supported by CNPQ 2013-SAU005.

## References

Atoui, J. A., Felipucci, D. N. B., Pagnano, V. O., Orsi, I. A., Nóbilo, M. A. A., & Bezzon, O. L. (2013). Tensile and flexural strength of commercially pure titanium submitted to laser and tugsten inert gas welds. *Brazilian Dental Journal*, 24(6):630-634. https://doi.org/10.1590/0103-6440201302241

Akman, E., Demir, A., Canel, T., & Sinmazçelik, T. (2009). Laser welding of Ti6Al4V titanium alloy. *Journal of Materials Processing Technology*, 209(8):3705-3713. https://doi.org/10.1016/j.jmatprotec.2008.08.026

Baba, N., & Watanabe, I. (2005). Penetration deph into dental casting alloys by Nd:YAG laser. *Journal of Biomedical Materials Research Part B: Applied Biomaterials*, 72(1):64-68. https://doi.org/10.1002/jbm.b.30117

Barbi, F. C. L., Camarini, E. T., Silva, R. S., Endo, E. H., & Pereira, J. R. (2012). Comparative analysis of different joining techniques to improve the passive fit of cobalt-chromium superstructures. *The Journal of Prosthetic Dentistry*, 108(6):377-385. https://doi.org/10.1016/S0022-3913(12)60196-6

Berg, E., Wagner, W. C., Davik, G., & Dootz, E. R. (1995). Mechanical properties of laser-welded cast and wrought titanium. *The Journal of Prosthetic Dentistry*, 74 (3):250-257. https://doi.org/10.1016/S0022-3913(05)80131-3

Byrne, G. (2011). Soldering in prosthodontics - an overview, part I. *Journal of Prosthodontics*, 20(3):233-243. https://doi.org/10.1111/j.1532-849X.2011.00691.x

Castro, G. C., Araújo, C. A., Mesquita, M. F., Consani, R. L. X., & Nóbilo, M. A. A. (2013). Stress distribution in Co-Cr implant frameworks after laser or TIG welding. *Brazilian Dental Journal*, 4(2):147-151. https://doi.org/10.1590/0103-6440201302112

Castro, M. G., Araújo, C. A., Menegaz, G. L., Lyra e Silva, J. P., Nóbilo, M. A. A., & Simamoto-Júnior, P. C. (2015). Laser and Plasma dental soldering techniques applied to Ti-6Al-4V alloy: Ultimate tensile strength and finite elemento analysis. *The Journal of Prosthetic Dentistry*, 113(5):460-466. https://doi.org/10.1016/j.prosdent.2014.10.008

Chai, T., & Chou, C. K. (1998). Mechanical properties of laser-welded cast titanium joints under different conditions. *The Journal of Prosthetic Dentistry*, 79(4):477-483. https://doi.org/10.1016/S0022-3913(98)70165-9

Kokolis, J., Chakmakchi, M., Theocharopoulos, A., Prombonas, A., & Zinelis, S. (2015). Mechanical and interfacial characterization of laser welded Co-Cr alloy with diferente joint configurations. *The Journal of Advanced Prosthodontics*, 7(1):39-46. https://doi.org/10.4047/jap.2015.7.1.39

Lyra e Silva, J. P., Fernandes Neto, A. J., Raposo, L. H. A., Novais, V. R., Araujo, C. A., Cavalcante, L. A. L., & Simamoto-Júnior, P.C. (2012). Effect of plasma welding parameters on the flexural strength of Ti-6Al-4V alloy. *Brazilian Dental Journal*, 23(6):686-691. https://doi.org/10.1590/S0103-64402012000600010

Matos, I. C., Bastos, I. N., Diniz, M. G., & Miranda, M. S. (2015). Corrosion in artificial saliva of a Ni-Cr-based dental alloy joined by TIG welding and conventional brazing. *The Journal of Prosthetic Dentistry*, 114(2):278-285. https://doi.org/10.1016/j.prosdent.2015.01.017

Nuñez-Pantoja, J. M. C., Takahashi, J. M. F. K., Nóbilo, M. A. A., Consani, R. L. X., & Mesquita, M. F. (2011). Radiographic inspection of porosity in Ti-6Al-4V laser-welded joints. *Brazilian Oral Research*, 25(2):103-108. https://doi.org/10.1590/S1806-83242011005000005

Nuñez-Pantoja, J. M. C., Farina, A. P., Vaz, L. G., Consani, R. L. X., Nóbilo, M. A.A., & Mesquita, M. F. (2012). Fatigue strength: effect of welding type and joint design executed in Ti-6Al-4V structures. *Gerodontology*, 29(2):e1005-e1010. https://doi.org/10.1111/j.1741-2358.2011.00598.x

Rocha, R., Pinheiro, A. L. B., & Villaverde, A. B. (2006). Flexural strength of pure Ti, Ni-Cr and Co-Cr alloys submitted to Nd:YAG laser or TIG welding. *Brazilian Dental Journal*, 17(1):20-23. http://dx.doi.org/10.1590/S0103-64402006000100005

Silveira-Júnior, C. D., Castro, M. G., Davi, L. R., Neves, F. D., Novais, V. R., & Simamoto-Júnior, P. C. (2012). Welding techniques in dentistry. In: Kovacevic R (Ed.), *Welding Processes*. (17a ed.), Croatia: In tech.

Simamoto-Júnior, P. C., Novais, V. R., Machado, A. R., Soares, C. J., & Raposo, L. H. A. (2015). Effect of joint design and welding type on the flexural strength and wel penetration of Ti-6Al-4V alloy bars. *The Journal of Prosthetic Dentistry*, 113(5):467-474. https://doi.org/10.1016/j.prosdent.2014.10.010

Takayama, Y., Nomoto, R., Nakajima, H., & Ohkubo, C. (2012). Effects of argon flow rate on laser-welding. *Dental Materials Journal*, 31(2):316-326.

https://doi.org/10.4012/dmj.2011-158

Takayama, Y., Nomoto, R., Nakajima, H., & Ohkubo, C. (2013) Comparasion of joint designs for laser welding of cast metal plates and wrought wires. *Odontology*, 101:34-42. https://doi.org/10.1007/s10266-011-0049-7

Taylor, J. C., Hondrum, S. O., Prasad A., & Brodersen C. A. (1998). Effects of joint configuration for the arc welding of cast Ti-6Al-4V alloy rods in argon. *The Journal of Prosthetic Dentistry*, 79(3):291-297. https://doi.org/10.1016/S0022-3913(98)70240-9

Wang, R. R., & Welsch, G. E. (1995). Joining titanium materials with tungsten inert gas welding, laser welding, and infrared brazing. *The Journal of Prosthetic Dentistry*, 74(5):521-530. https://doi.org/10.1016/S0022-3913(05)80356-7

Watanabe, I., & Topham, D. S. (2006). Laser welding of cast titanium and dental alloys using argon shielding. Journal of Prosthodontics, 15(2):102-107. https://doi.org/10.1111/j.1532-849X.2006.00082.x

Zupancic, R, Legat, A., & Funduk, N. (2006). Tensile strength and corrosion resistance of brazed and laser-welded cobalt-chromium alloy joints. *The Journal of Prosthetic Dentistry*, 96(4):273-282. https://doi.org/10.1016/j.prosdent.2006.08.006